PCCP

Physical Chemistry Chemical Physics

www.rsc.org/pccp

Volume 10 | Number 48 | 28 December 2008 | Pages 7189–7336

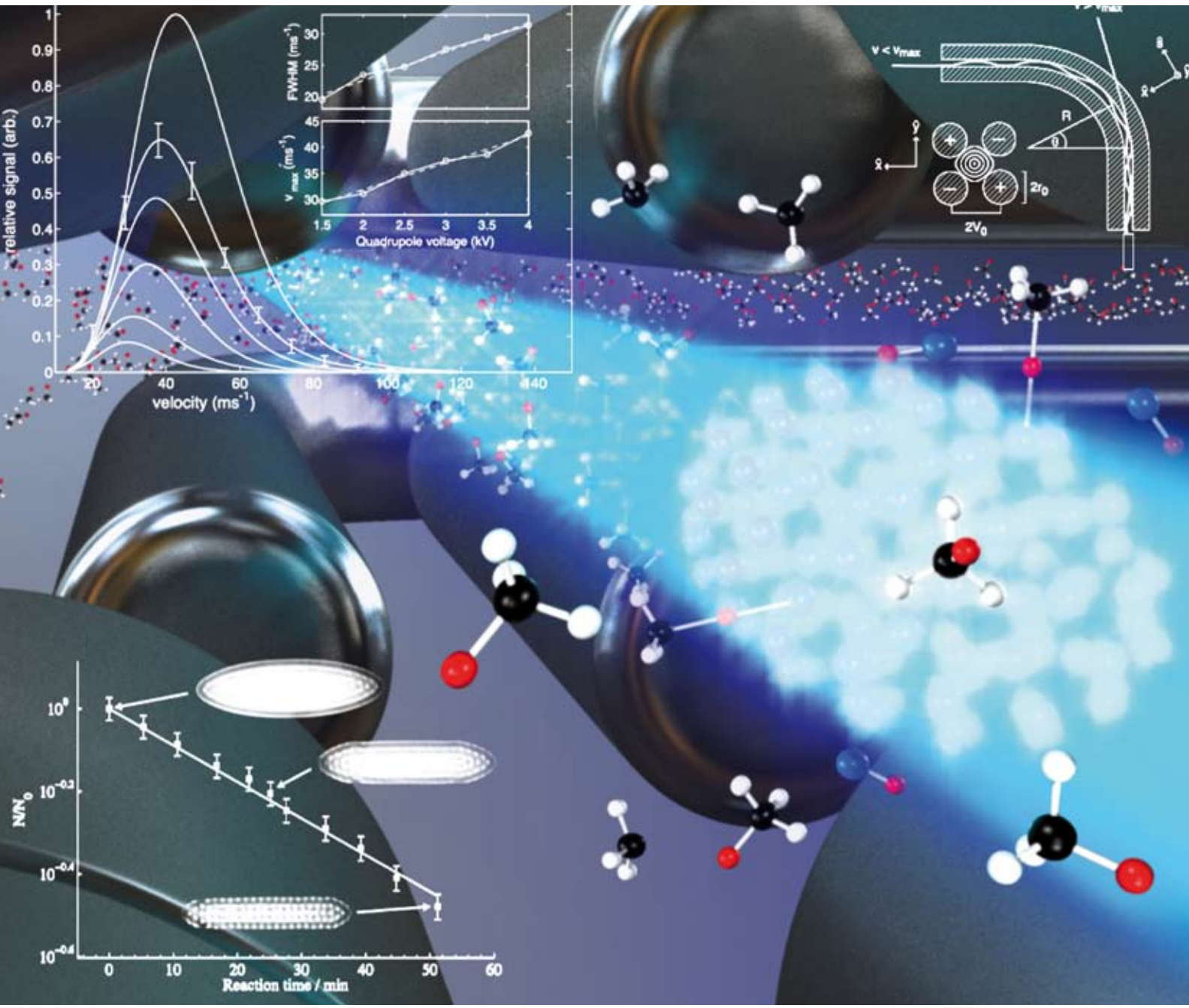

ISSN 1463-9076

COVER ARTICLE
Willitsch *et al.*
Chemical applications of laser- and sympathetically-cooled ions in ion traps

PERSPECTIVE
Woodruff
The interface structure of n-alkylthiolate self-assembled monolayers on coinage metal surfaces

1463-9076(2008)10:48;1-R

Chemical applications of laser- and sympathetically-cooled ions in ion traps

Stefan Willitsch,†*[ab] Martin T. Bell,[c] Alexander D. Gingell[c] and Timothy P. Softley[c]

Received 1st August 2008, Accepted 1st September 2008
First published as an Advance Article on the web 22nd October 2008
DOI: 10.1039/b813408c

Ensembles of cold atomic and molecular ions in ion traps prepared at millikelvin temperatures by laser and sympathetic cooling have recently found considerable interest in both physics and chemistry. At very low temperatures the ions form ordered structures in the trap also known as "Coulomb crystals". Ion Coulomb crystals exhibit a range of intriguing properties which render them attractive systems for novel experiments in chemical dynamics, ultrahigh-resolution spectroscopy and quantum-information processing. In this article we review the methods used to prepare atomic and molecular ion Coulomb crystals and discuss some recent studies in mass spectrometry, low-temperature chemistry and precision spectroscopy to illustrate their scientific potential for chemical applications. Finally, we conclude with an outlook on outstanding challenges and prospective further developments in the field.

1. Introduction

The preparation and study of atomic and molecular matter at very low temperatures ($T \lessapprox 1$ K) in the gas phase is presently one of the most vibrant fields in physics and physical chemistry. The considerable interest in this topic stems from the unusual properties of cold matter and its many potential applications. The large thermal de Broglie wavelengths at very low temperatures lead to phenomena such as Bose–Einstein condensation,[1] the formation of Fermi gases[2] and profoundly influence the chemical dynamics.[3–5] Moreover, cold atoms and molecules have been identified as attractive systems for quantum-information processing[6–8] and ultrahigh-resolution spectroscopy[9] with the aim of developing new time standards[10] and to test fundamental physical theories such as the time variation of physical constants[11,12] or the existence of a dipole moment of the electron.[13]

A particularly interesting form of cold matter is ordered structures of strongly localized ions in ion traps (see Fig. 1). These structures are usually referred to as "Coulomb crystals" or "Wigner crystals"[14] by analogy to ordered arrangements of electrons in solids originally predicted by Wigner in 1934.[15] Coulomb crystals exhibit a range of intriguing properties. First, the ions are translationally cold (down to millikelvins or even lower). Second, because of their strong localization it is possible to observe and manipulate individual ions enabling experiments with single-particle sensitivity. Third, the ion trap situated in an ultrahigh-vacuum chamber constitutes a well-defined experimental environment in which external perturbations such as stray fields and collisions with background gas molecules can be minimized to provide ideal conditions for precision studies. Fourth, ion Coulomb crystals can be stored for hours, even years in the case of single ions, enabling experiments with very long interaction and observation times.

An ion Coulomb crystal can be regarded as a strongly coupled non-neutral plasma[16,17] whereby the degree of coupling is quantified by the plasma coupling parameter Γ defined as the ratio of kinetic to potential energy

$$\Gamma = \frac{E_{\mathrm{pot}}}{E_{\mathrm{kin}}} = \frac{Q^2}{4\pi\varepsilon_0 a_{\mathrm{WS}} k_{\mathrm{B}} T}. \qquad (1)$$

In eqn (1), Q is the charge of the ion, T is the temperature and a_{WS} stands for the Wigner–Seitz radius which is a measure of the inter-ion distance given by $a_{\mathrm{WS}} = [3/(4\pi n)]^{1/3}$ where n is the particle density.[16] Monte-Carlo and molecular-dynamics simulations[18,19] as well as experimental studies[20,21] have

[a] *Department of Chemistry, University College London, 20 Gordon Street, London, UK WC1H 0AJ*
[b] *Department Chemie, Universität Basel, Klingelbergstrasse 80, 4056 Basel, Switzerland*
[c] *Department of Chemistry, University of Oxford, Chemistry Research Laboratory, Mansfield Road, Oxford, UK OX1 3TA*
† Present address: Universität Basel. *E-mail:* stefan.willitsch@unibas.ch.

Stefan Willitsch

Stefan Willitsch graduated in natural sciences from the Eidgenössische Technische Hochschule (ETH) Zürich (Switzerland) in 2000 and received his PhD from the Laboratory of Physical Chemistry of ETH in 2004. In the same year he joined Christ Church College and the Physical and Theoretical Chemistry Laboratory at the University of Oxford (UK) as a Junior Research Fellow. He was appointed lecturer at University College London (UK) in 2007 and since 2008 he is an assistant professor at the Department of Chemistry at the University of Basel (Switzerland).

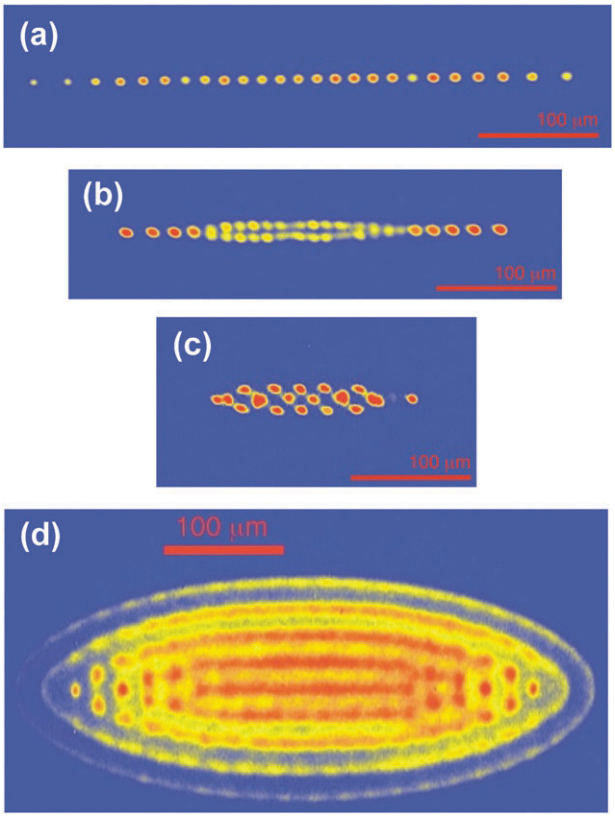

Fig. 1 (a–c) False-colour fluorescence images of the spatial arrangement of 25 laser-cooled Ca^+ ions in a Coulomb crystal recorded under varying trapping conditions. (a) A string of ions (V_{END} = 1.6 V), (b) a helix (V_{END} = 2.4 V), (c) a spheroid (V_{END} = 5.4 V). The RF frequency $\Omega_{RF} = 2\pi \times 3.9$ MHz and RF amplitude $V_{RF,0}$ = 200 V was held constant in all three measurements. (d) False-colour fluorescence image of a large spheroidal Coulomb crystal consisting of hundreds of Ca^+ ions.

shown that the ions undergo a phase transition to an ordered state if $\Gamma \approx 150$. It follows from eqn (1) that this transition occurs around temperatures of tens of mK at the typical inter-ion distances of tens of μm prevalent in Coulomb crystals.

Such low temperatures can only be reached using laser cooling whereby optical forces are used to slow down the ions.[22] This technology is to be contrasted with cryogenic buffer-gas-cooling methods which are nowadays widely used to prepare cold ($T \gtrapprox 4$ K) samples of ions for chemical[23] and spectroscopic studies.[24,25] However, as laser cooling is generally not applicable to molecules because of the lack of closed optical cycles, atomic-ion Coulomb crystals have thus far mainly found applications in the world of physics, particularly in quantum-information processing where they are used as a framework for the implementation of quantum-logic protocols.[6,26–28] This situation has changed only recently with the advent of methods to sympathetically cool molecular ions down to mK temperatures using the Coulomb interaction with laser-cooled atomic ions.[29,30] The development of these techniques enabled the generation of molecular Coulomb crystals thus establishing a link between the field of cold ions and the study of molecular phenomena.

The aim of this article is to review the recent progress in the generation of atomic and molecular ion Coulomb crystals, to discuss their properties, and to highlight some recent experiments in mass spectrometry, low-temperature chemistry and high-resolution spectroscopy which demonstrate the potential of cold ions for novel applications in a chemical context.

2. Generation and properties of cold ions

2.1 The linear Paul trap

The most common type of ion trap used to prepare ion Coulomb crystals is the linear Paul trap,[31–33] although Penning traps,[34,35] octupole traps[36] and, more recently, microfabricated radiofrequency (RF) traps on chips[37] have been used as well. As shown in Fig. 2(a), a linear Paul trap typically consists of four segmented cylindrical electrodes arranged in a quadrupolar configuration to generate an approximately harmonic electric potential close to the centre of the trap.[38–40] Because the Laplace equation forbids the existence of a static potential minimum in three-dimensional charge-free space, the ions are confined by applying RF and direct-current (DC) voltages to the different segments of the trap electrodes as indicated in Fig. 2(a). The RF voltages are of the form $V_{RF}(t) = \pm V_{RF,0} \cos(\Omega_{RF} t)$ where $V_{RF,0}$ denotes the RF amplitude, t is the time and $\Omega_{RF} = 2\pi f_{RF}$ whereby f_{RF} is the RF frequency. The polarity of the RF voltage alternates between adjacent rods to create a potential saddle point at the centre of the trap. The orientation of the saddle point periodically flips between the x and y directions to dynamically

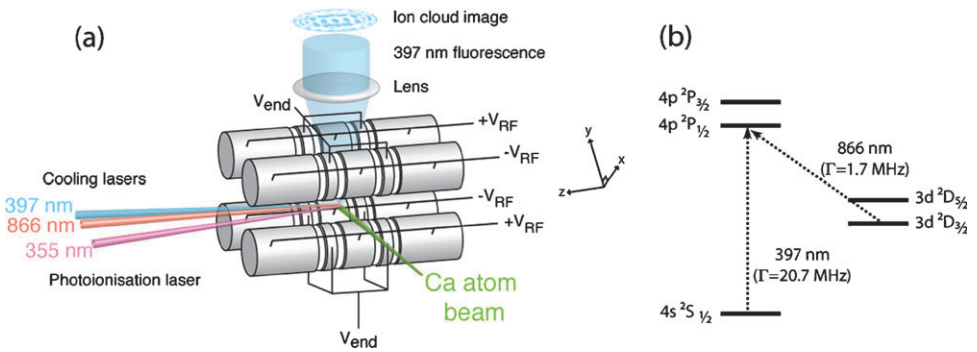

Fig. 2 (a) Schematic representation of the laser cooling of ions in a linear Paul trap, see text for details. (b) Diagram of the relevant energy levels used in Doppler laser cooling of $^{40}Ca^+$.

confine the ions in the x, y plane perpendicular to the trap (z) axis. Trapping in the z direction is achieved by applying a static voltage V_{end} to the endcap segments of the trap electrodes. The resulting equations of motions for a single ion in a linear Paul trap assume the form of the Mathieu equations[32,33,38]

$$\frac{\mathrm{d}^2u}{\mathrm{d}\tau^2} + [a_u + 2q_u\cos(2\tau)]u = 0 \qquad (2)$$

with $u \in \{x, y, z\}$ and $\tau = (1/2)\Omega_{\mathrm{RF}}t$. The solutions of eqn (2) have been discussed in the literature, see, *e.g.*, ref. 31–33. Stable confinement of the ion depends only on the values of the Mathieu parameters

$$a_x = a_y = -\frac{1}{2}a_z = -\kappa\frac{4QV_{\mathrm{end}}}{m\Omega_{\mathrm{RF}}^2 z_0^2} \qquad (3)$$

$$q_x = -q_y = \frac{2QV_{\mathrm{RF},0}}{m\Omega_{\mathrm{RF}}^2 r_0^2},\ q_z = 0 \qquad (4)$$

where $2z_0$ is the separation of the endcaps of the trap, m is the mass of the ion, r_0 is the closest distance from the central trap axis to the surface of the electrodes and κ is a factor related to the geometry of the ion trap. The regions of stable confinement in (a, q) space are commonly represented in the form of stability diagrams.[33,38,39]

It is insightful to analyse the motion of an ion in a RF trap in terms of an adiabatic approximation, see ref. 40, 41 for a detailed discussion. The rapidly alternating RF voltages cause a fast periodic "micromotion" which is distinct from the slow thermal motion of the ions (also referred to as "secular motion"). The velocity of the micromotion increases proportionally with the distance from the central trap axis reflecting the increasing electric field strengths in the direction of the trap electrodes. In the adiabatic regime the fast micromotion can be separated from the slow secular motion. The time-averaged kinetic energy stored in the micromotion gives rise to a time-independent pseudopotential V^* which confines the ions in the x, y plane.[40] For a quadrupole trap, the pseudopotential function is harmonic and is given by ref. 33

$$V^*(r,z) = \tfrac{1}{2}\omega_r^2 r^2 + \tfrac{1}{2}\omega_z^2 z^2 \qquad (5)$$

with

$$r = \sqrt{x^2 + y^2}$$

and ω_r and ω_z are the radial and axial secular frequencies of the ion in the pseudo-potential well given by

$$\omega_i = \sqrt{a_i + (1/2)q_1^2}. \qquad (6)$$

The pseudo-potential model adequately describes the trajectories of the thermal motion of the ions, allows the establishment of conditions for stable trapping and can be extended to include space–charge phenomena, but does not include time-dependent effects induced by the oscillating RF fields.[38,39]

2.2 Doppler laser cooling

Doppler laser cooling of atoms, including atomic ions, is achieved by repeated absorption and spontaneous-emission cycles on a closed optical transition using a narrow-bandwidth continuous laser source, whereby the transfer of momentum upon the absorption of a photon is used to slow down the atoms.[22] Cooling can be achieved by slightly red-shifting the frequency of the laser beam with respect to the optical transition frequency. In this case only atoms with a velocity component opposite to the direction of propagation of the laser beam absorb photons; for these atoms the Doppler shift compensates the mismatch between the laser and the transition frequency. Thus only "head-on" collisions between atoms and photons lead to a transfer of momentum and a decrease of the atom's velocity. Whereas for neutral atoms a total of six beams are necessary to cool in positive and negative directions along the x, y and z axes, the implementation of laser cooling is considerably simpler for trapped ions; cooling can be achieved with a minimum of one laser beam because all translational degrees of freedom are coupled by the potential of the ion trap.

Ions commonly used in laser-cooling experiments are systems with a simple "alkali-like" energy-level structure such as the singly charged alkaline-earth ions Be^+,[42,43] Mg^+,[44] Ca^+,[27,45] and Ba^+[46] among others. In our laboratory Ca^+ is used which exhibits a favourable mass-to-charge ratio for the efficient sympathetic cooling of small to medium-sized molecular ions (see section 5) and which can be laser cooled with a comparatively small experimental effort using standard diode-laser technology. A diagram showing the relevant energy levels used for Doppler laser cooling in Ca^+ is given in Fig. 2(b). A schematic experimental setup is depicted in Fig. 2(a). Doppler laser cooling is performed on the $4s\ ^2S_{1/2} \rightarrow 4p\ ^2P_{1/2}$ transition at a wavelength of 397 nm. Because the $4p\ ^2P_{1/2}$ level can also decay to the metastable $3d\ ^2D_{3/2}$ state by spontaneous emission with a branching ratio of about 1 : 12, an additional laser beam at 866 nm is required to re-pump population shelved in the $3d\ ^2D_{3/2}$ level in order to close the laser cooling cycle. The Ca^+ ions are produced by photoionisation of a thermal beam of Ca atoms using the frequency-tripled output (355 nm) of a pulsed Nd:YAG laser.

The lowest translational temperature which can be achieved with this simple Doppler cooling scheme corresponds to

$$T_{\mathrm{min,\ Doppler}} = \frac{\hbar\Gamma}{2k_{\mathrm{B}}}, \qquad (7)$$

where Γ is the linewidth of the laser-cooling transition. For the 397-nm Doppler cooling transition in Ca^+ one obtains $T_{\mathrm{min,Doppler}} = 0.5$ mK. Fundamentally, the minimum achievable temperature is limited by the zero-point kinetic energy of the motion of the ion in the potential of the ion trap, *i.e.*, the zero-point energies corresponding to the motional frequencies ω_z and ω_r in eqn (5). Cooling to the vibrational ground state requires more elaborate schemes under conditions where the individual motional levels of the ions are resolved, see, *e.g.*, ref. 27, 47 and references cited therein.

2.3 Coulomb crystals

Fig. 1 shows a series of fluorescence images of Coulomb crystals consisting of 25 Ca^+ ions recorded under different trapping conditions. The images were obtained by monitoring the spontaneous emission of the ions (generated through the continuous absorption and emission cycles of the laser cooling process) using a microscope coupled to a CCD camera. The

fluorescence intensity is colour-coded ranging from low (blue) to high (red). The images show the time-averaged motion of the laser-cooled Ca^+ ions. At low axial trapping voltages V_{end}, the ions arrange in a string (Fig. 1(a)). In this configuration the ions are strongly localized and every bright spot indicates the position of a single Ca^+ ion. With increasing V_{end} the ions assume helical (Fig. 1(b)) and finally three-dimensional (Fig. 1(c)) structures. Large three-dimensional crystals consisting of hundreds of ions such as the one displayed in Fig. 1(d) generally exhibit spheroidal shapes because of the symmetry of the trapping potential eqn (5). In crystals of this size only a slice through the three-dimensional object is observed in the images because of the narrow focal depth of the imaging system.

Under typical trapping conditions (in our setup $V_{RF,0}$ = 150–250 V, $\Omega_{RF} = 2\pi \times 4$ MHz, V_{end} = 1–5 V), the distances between the ions are of order tens of microns. From the images in Fig. 1 it also becomes evident that the term "crystal" is strictly speaking a misnomer because the ions do not form a regular lattice as a consequence of the harmonic trapping potential. Periodic structures of ions which exhibit true translational symmetry have only been observed in very large ensembles (>1000 ions) in RF[48] and Penning traps.[34]

An important feature of RF traps is that laser cooling only affects the secular motion of the ions and not the micromotion which is constantly driven by the RF fields. In the adiabatic regime the ions exhibit two different kinetic-energy scales corresponding to these two types of motions. Whereas the secular kinetic energies obey a Maxwell–Boltzmann distribution with corresponding temperatures as low as millikelvins under Doppler-cooling conditions, the kinetic energies associated with the micromotion are considerably higher and determined by the RF fields at the position of the relevant ion in the trap.[49–52] Because the RF field strength increases linearly from the central trap axis, the sample of ions does not have a uniform temperature distribution and effective ion kinetic energies (expressed as an equivalent temperature) can be as high as tens of Kelvins depending on the RF amplitudes and the distance of the ion from the trap axis. The shape and morphology of the Coulomb crystals are almost exclusively governed by the properties of the time-averaged pseudopotential eqn (5)[19,49,51]—indeed, in the adiabatic regime the point of transition to the ordered "crystalline" structure is solely dependent on the temperature T_{sec} associated with the secular motion.[50] On the other hand the effective kinetic energies of the ions are dictated by the fully time-dependent trap potential which gives rise to the micromotion.[52] This distinction is particularly important in experiments which probe the effective kinetic energy of the ions, *e.g.*, reactive-scattering experiments (see section 3.2).

2.4 Molecular-dynamics simulations of cold ions

Molecular-dynamics simulations represent a powerful tool for the theoretical study of the structure, properties and dynamics of ion Coulomb crystals. Because the motion of the ions in the trap behaves classically when the individual motional levels of the ions are not resolved,[47] the trajectories of the individual particles can be obtained by solving Newton's equation of motion.[49–52] The force acting on a single ion in an ensemble can be formulated as

$$F_{i,tot} = F_{trap} + F_{Coulomb} + F_{LC} + F_{heating}, \quad (8)$$

where the individual terms describe the harmonic trapping force, the Coulomb force between the ions, the laser-cooling force and a stochastic force which is introduced to effectively take into account the heating of the ions caused by collisions and by imperfections in the trap geometry and RF fields. The heating force is computationally implemented by imparting random velocity kicks of a defined magnitude to the ions at every time step in the simulation. The first term on the right-hand side of eqn (8) corresponds to the Mathieu equations given by eqn (2). The Coulomb term is given by

$$F_{Coulomb} = \frac{Q_i}{4\pi\varepsilon_0}\nabla_i\left[\sum_{i\neq j}\frac{Q_j}{r_{ij}}\right], \quad (9)$$

where r_{ij} is the distance between ions i and j and ∇_i is the Nabla operator. Finally, the velocity-dependent laser-cooling force along the positive z-axis can be expressed as $F_{LC} = -\beta\dot{z}$ where β is a damping coefficient.[22]

From the trajectories of the ions, simulated fluorescence images of the Coulomb crystals can be generated. A comparison between experimental and simulated images can then be used to determine the number of ions in large crystals and to study the shape and composition of multi-component crystals. Moreover, the images sensitively depend on the secular temperature of the ions as higher temperatures lead to a blurring of the images as a consequence of the increased mobility of the ions. The effective kinetic energies on the other hand cannot be directly inferred from the images because the amplitude of the micromotion is generally too small to be observable (the resolution of typical imaging systems is on the order of one micrometer). In this case MD simulations are the only means by which to establish the effective kinetic energy distributions of the ions.[51,52]

2.5 Sympathetic cooling and molecular Coulomb crystals

In general, laser cooling cannot be applied to molecules because their complex energy-level structure precludes the implementation of closed optical cycles. However, an alternative method to produce samples of molecular ions at millikelvin temperatures is sympathetic cooling. When molecular ions are simultaneously trapped with laser-cooled atomic ions, the Coulomb interaction ensures efficient transfer of kinetic energy from the molecular to the atomic species from which it is constantly removed by the optical forces. As a result, a bi-component or "molecular" Coulomb crystal is formed in which both types of ions form ordered structures with secular temperatures down to millikelvins. The first sympathetic-cooling experiments of molecular ions by laser-cooled ions were performed by Baba and Waki in 1996.[29] The technique has subsequently been refined and extended by the groups of Drewsen, Schiller and Thompson, see, *e.g.*, ref. 30, 43, 53, 54 and references cited therein.

Fig. 3(a) shows a bi-component Coulomb crystal consisting of laser-cooled Ca^+ and sympathetically cooled CaF^+ ions. Because the effective trap potential is deeper for the lighter

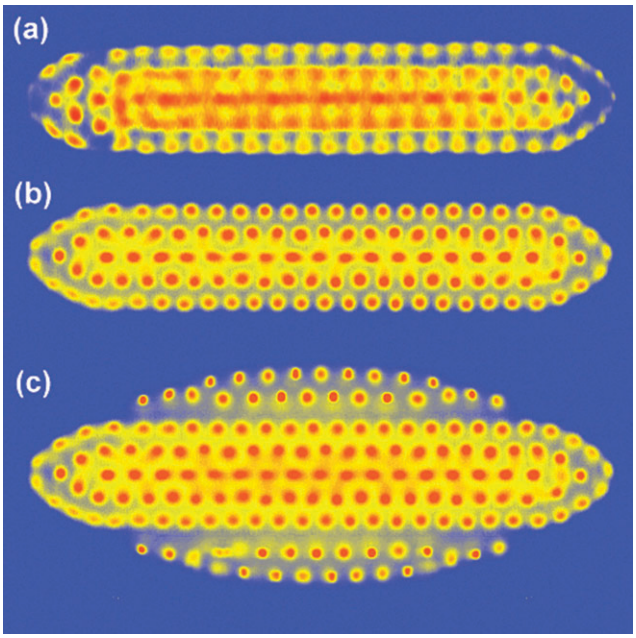

Fig. 3 False-colour fluorescence images of a Ca^+/CaF^+ bi-component Coulomb crystal. (a) Experimental image of the central core of laser-cooled Ca^+ ions. The CaF^+ ions do not exhibit laser-induced fluorescence at the laser wavelengths used in the experiment and are thus not observed in the image. (b) Synthetic fluorescence image of the central core of Ca^+ ions created from a MD simulation of the ion trajectories. (c) As (b) with the non-fluorescing CaF^+ ions made visible in the construction of the image.

species, the Ca^+ ions accumulate near the trap centre and are surrounded by the heavier non-fluorescing molecular ions, which cannot be directly observed in the images.[55] However, their presence manifests itself as a deformation of the central Ca^+ core whose shape markedly deviates from the spheroids usually observed in single-component crystals like the one displayed in Fig. 1(d). This is confirmed by the synthetic image Fig. 3(b) which has been generated from molecular-dynamics simulations of the crystal shown in Fig. 3(a). Fig. 3(c) shows the same simulated crystal whereby the sympathetically cooled CaF^+ ions have been made visible in the reconstruction of the image.

Sympathetic cooling has extensively been studied both experimentally and theoretically.[29,30,43,44,46,51,54–59] Energy transfer between laser- and sympathetically cooled species is most efficient between ions of equal mass-to-charge ratio. The heaviest species for which sympathetic cooling has thus far been achieved are organic dye molecules with a mass exceeding 400 amu‡.[54] In these experiments $^{138}Ba^+$ was employed as the coolant ion.

Sympathetic cooling of ions is mediated by the long-range Coulomb interaction at inter-particle distances of tens of microns typical for trapped ions. Higher-order interactions that can induce inelastic processes, such as electric-dipole coupling, are only effective on considerably shorter length scales and can be neglected in a Coulomb crystal. Hence, sympathetic cooling does not affect the internal degrees of freedom of the molecules which are usually in thermal equilibrium with the ambient black-body radiation field.[60,61]

3. Selected applications

3.1 Mass spectrometry and single-ion chemistry

The secular motional frequencies of the trapped ions are a function of the mass of the ion (see eqn (6), (3) and (4)) and so a measurement of the secular frequencies offers a means for mass spectrometry of the trapped particles. In ion-trap mass spectrometers, this is usually achieved by applying an additional RF drive voltage to the trap electrodes.[38] If the RF drive frequency is in resonance with the secular oscillation frequency of the ions in the trap, the relevant motion is excited and the ions are ejected from the trap at sufficiently high drive amplitudes. A mass spectrum is obtained by monitoring the yield of ejected ions as a function of the drive frequency.

A non-destructive variation of this resonant-excitation technique has been developed and was first described by Baba and Waki in 1996 who also coined the term "sympathetically laser-cooled fluorescence mass spectrometry".[29] The method relies on the modulation of the fluorescence intensity of the laser-cooled ions as a consequence of the excitation of the secular motion of any of the trapped species. If the secular motion of a trapped ion species is excited, the Coulomb interaction ensures an efficient transfer of kinetic energy to the laser-cooled ions. Consequently, the ions heat up and are Doppler-shifted out of resonance with the cooling laser, thus resulting in a decrease of the laser-cooling fluorescence intensity. A mass spectrum is obtained by measuring the fluorescence yield as a function of the drive frequency. Dips in the fluorescence-yield curve indicate the positions of the motional resonances. As only weak RF drive fields are required, the ions are not ejected from the trap enabling a non-destructive *in situ* mass analysis of the trapped species. A variation of this method was developed by Schiller and co-workers whereby the cooling laser is far detuned, and resonant excitation Doppler-shifts the absorption frequency of the ions closer to the laser-cooling transition.[46] In this scheme an increase of the fluorescence yield is indicative of resonant excitation.

As an example, Fig. 4(c) shows the resonant-excitation mass spectrum of a one-component Coulomb crystal consisting of 15 Ca^+ ions (Fig. 4(a)). One resonance is observed in the spectrum corresponding to the excitation of the centre-of-mass motion of the Ca^+ ions. After replacing a fraction of the Ca^+ ions in the crystal with CaF^+ ions (Fig. 4(b)), the spectrum in panel (d) is obtained which shows two types of resonances corresponding to the excitation of the CaF^+ and Ca^+ species, respectively.

In crystallized ensembles, the strong Coulomb coupling between the closely spaced ions causes a marked dependence of the positions and widths of the motional resonances on the trapping parameters, the number of ions and the composition of the sample.[57,62] This can readily be seen by comparing the mass spectra shown in Fig. 4(c) and (d). In the spectrum of the

‡ Note added in proofs: Since the preparation of this manuscript, the sympathetic cooling of multiply charged cytochrome *c* proteins with a mass of approximately 12390 amu has been reported (S. Schiller, private communication).

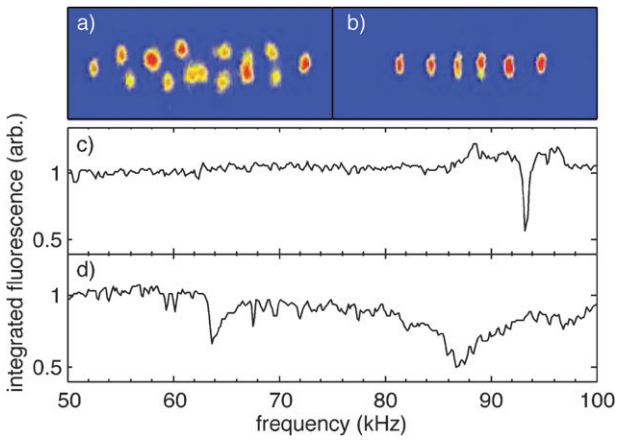

Fig. 4 False-colour fluorescence images of (a) a Coulomb crystal of 15 Ca^+ and (b) a small Ca^+/CaF^+ bi-component crystal. (c) Resonant-excitation mass spectrum of the crystal in (a). The resonance observed corresponds to the motional excitation of the Ca^+ ions. (d) Resonant-excitation mass spectrum of the crystal in (b). The two features in the spectrum are assigned to the excitation of CaF^+ and Ca^+ ions, respectively. The shift and broadening of the Ca^+ peak in the bi-component crystal is caused by the Coulomb interaction between the different ion species, see text for details. Adapted from Willitsch *et al.*[45]

bi-component crystal shown in (d), the position and width of the Ca^+ resonance markedly differ from the one observed for the pure crystal (c) as a consequence of the space-charge drag of the two ion species on one another. Thus, resonant-excitation mass spectra of larger many-component crystals are usually poorly resolved and depend strongly on the experimental conditions.

The situation is fundamentally different in a two-ion crystal consisting of one laser-cooled and one sympathetically cooled ion. In such systems a significantly higher resolution in laser-cooled fluorescence mass spectrometry can be achieved as was recently demonstrated by Drewsen *et al.*[63] A Coulomb crystal consisting of only two ions has six motional degrees of freedom, which can be described in terms of normal modes. Two modes are directed along the trap axis: the centre-of-mass mode ν_-, in which the ions oscillate in phase, and a breathing or symmetric stretching mode, ν_+. Assuming a harmonic trap potential, the frequencies of these two modes can be calculated analytically and are given by ref. 63

$$\nu_\pm^2 = \left[(1 + m_1/m_2) \pm \sqrt{1 - m_1/m_2 + (m_1/m_2)^2}\right]\nu_1^2, \quad (10)$$

where m_1 and m_2 stand for the masses of the two ions and ν_1 is the frequency of the single ion of mass m_1. If one of the masses, say the mass of the laser-cooled ion m_1, is already known, the measurement of either ν_+ or ν_- enables the determination of the mass of the sympathetically cooled ion m_2.

Drewsen *et al.* employed two different experimental approaches to determine ν_- and thereby m_2.[63] Using a conventional RF resonant-excitation scheme with laser-cooling fluorescence detection, a mass resolution of order $\Delta m/m \approx 10^{-2}$ was achieved that was limited by the damping of the ion motion caused by the electric and optical fields. An alternative method, which is less sensitive to damping effects, consists of inducing resonant excitation by optical forces and detecting only the component of the ion motion in phase with the periodic perturbation. This was achieved by a modulation of the laser-cooling force whereby one of the cooling-laser beams was chopped at a variable frequency. The spatially resolved fluorescence of the laser-cooled ion was measured in phase with the modulation frequency thus yielding a dispersion-type shape of the resonance, see Fig. 5. The motional frequency was determined from the zero-crossing of the signal resulting in a considerably improved accuracy. In the two-ion system consisting of a laser-cooled $^{40}Ca^+$ and a sympathetically cooled $^{42}Ca^+$ ion displayed in Fig. 5(b) a mass resolution of $\Delta m/m \approx 10^{-4}$ was achieved with this method.

Although this resolution does not rival that achievable in recent mass-spectrometric experiments using Penning traps,[64] it is amply sufficient to track chemical changes of the sympathetically cooled ion over the course of an experiment without the need to eject and thereby destroy the trapped particles. Indeed, this analytical method proved particularly useful in the study of chemical processes at the single-particle level thus reaching the ultimate limit of sensitivity in gas-phase chemistry.

Højbjerre *et al.*[65] investigated the sequential photodissociation of single aniline ions $C_6H_5NH_2^+$. The aniline ions were produced by resonance-enhanced two-photon ionization with a pulsed laser at 294 nm, resonant with the vibrationless $S_0 \rightarrow S_1$ transition of the neutral molecule. After sympathetic cooling of a single aniline ion by a single Ca^+ ion into a two-ion crystal, the aniline ion was subjected to photodissociation by the 397 nm cooling and 294 nm photodissociation laser beams. While the ion was irradiated by the laser beams, resonant-excitation mass spectra (as described above) were recorded at fixed time intervals to periodically measure the mass of the sympathetically cooled ion. It was found that under the

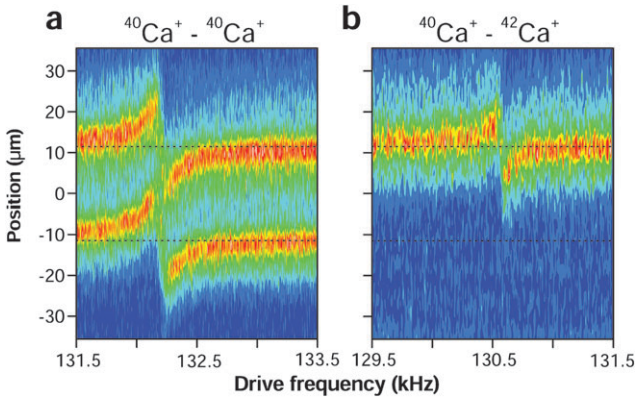

Fig. 5 High-resolution resonant-excitation mass spectra of (a) $^{40}Ca^+$–$^{40}Ca^+$ and (b) $^{40}Ca^+$–$^{42}Ca^+$ two-ion Coulomb crystals. The images were obtained by modulating the laser cooling force and measuring the ion fluorescence in phase with the perturbing force. From the dispersion-shaped fluorescence signatures, the mass of the sympathetically cooled ions can be determined with a relative accuracy of $\approx 10^{-4}$. Reproduced from Drewsen *et al.*[63] Copyright 2004 by the American Physical Society.

experimental conditions used the aniline ions undergo a series of consecutive photodissociation and isomerization processes according to the series $C_6H_5NH_2^+ \rightarrow C_5H_6^+ \rightarrow C_5H_5^+ \rightarrow C_3H_3^+$.

Such studies of chemical reactions of single ions are not only restricted to unimolecular processes. Staanum *et al.*[66] studied the isotopic branching ratio of the bimolecular reaction of electronically excited Mg^{+*} ions with HD molecules to yield MgH^+ and MgD^+:

$$Mg^{+*} + HD \rightarrow MgH^+ + D \text{ [Channel 1]} \quad (11)$$

$$\rightarrow MgD^+ + H \text{ [Channel 2]} \quad (12)$$

by monitoring the production of single product ions. In these experiments, a system of two laser-cooled Mg^+ ions was prepared before leaking HD gas into the UHV chamber. The HD pressure was kept sufficiently low so that only one of the Mg^+ ions would react at a time to form a product ion which remained trapped and whose mass was measured by resonant-excitation mass spectrometry. By averaging over $\approx$300 single-ion reaction experiments, the branching ratio between Channels 1 and 2 was found to be 1 : 5.

3.2 Cold ion-molecule chemistry

One of the most intriguing applications of cold molecular ions is the study of chemical reactions at very low temperatures $T \lesssim 1$ K. Theoretical calculations predict that the chemical reactivity at ultralow collision energies is dominated by quantum effects such as reactive resonances, s-wave reactive scattering and tunnelling through low-lying energy barriers which are often not observed at higher temperatures because of thermal averaging.[4,67–69] The study of these effects enables the probing of the details of the reaction mechanism and the topology of the relevant potential energy surface, especially the long-range region, and provides stringent tests of high-level *ab initio* and reactive-scattering calculations.

The experimental realization of reactive-collision studies between neutral molecules at temperatures near 1 K or below has proved challenging on the grounds of the low number densities which can be produced with present-day cold-molecules sources (typically of order 10^6–10^8 molecules cm^{-3}). Indeed, at such low number densities it is to be expected that only a small number of reactive collisions occur in every experimental cycle, the detection of which represents a severe experimental challenge. In contrast to neutral species, cold trapped ions are strongly localized and can be observed and manipulated at the single-particle level thus offering the possibility to study cold reactive collisions with sufficient sensitivity even at low number densities.

The first experiment of this kind was recently developed in our laboratory and allows the study of chemical reactions between Coulomb-crystallized ions and translationally-cold neutral molecules down to temperatures of about 1 K.[45] The apparatus consists of a linear Paul trap for the laser cooling of Ca^+ ions combined with a quadrupole-guide velocity selector to produce continuous beams of slow polar neutral molecules.

The cold neutrals are produced by selecting the slowest molecules from the Maxwell–Boltzmann distribution of a thermal sample at $T = 298$ K, as first demonstrated by Rempe and coworkers.[70] An effusive molecular beam with a backing pressure of $p \approx 0.1$ mbar is coupled into a bent electric quadrupole. The electrodes are charged to high voltage (V_{QUAD} = 2–5 kV) with alternating polarities between adjacent rods to generate a strong quadrupolar electric field in the centre of the guide. Molecules in low-field seeking Stark states, *i.e.*, states whose Stark energy increases with increasing field strength, are trapped in the centre of the guide where there is a local field minimum, whereas molecules in high-field seeking states are pushed out of the quadrupole. When reaching the bend, only the slowest molecules are forced around the corner whereas fast molecules are lost from the guide. Because, in general, a range of different Stark components is guided, the velocity-selected molecules are translationally-cold but exhibit a distribution of rotational states.[52,71,72]

The guided flux and mean kinetic energy of the velocity-selected molecules is dependent on the voltage applied to the electrodes. Higher potentials lead to less restrictive velocity filtering because a larger part of the thermal distribution of molecules is guided, but also result in an increased guided flux. With this method continuous beams of cold neutral molecules with average kinetic energies (defined as the mean value of the

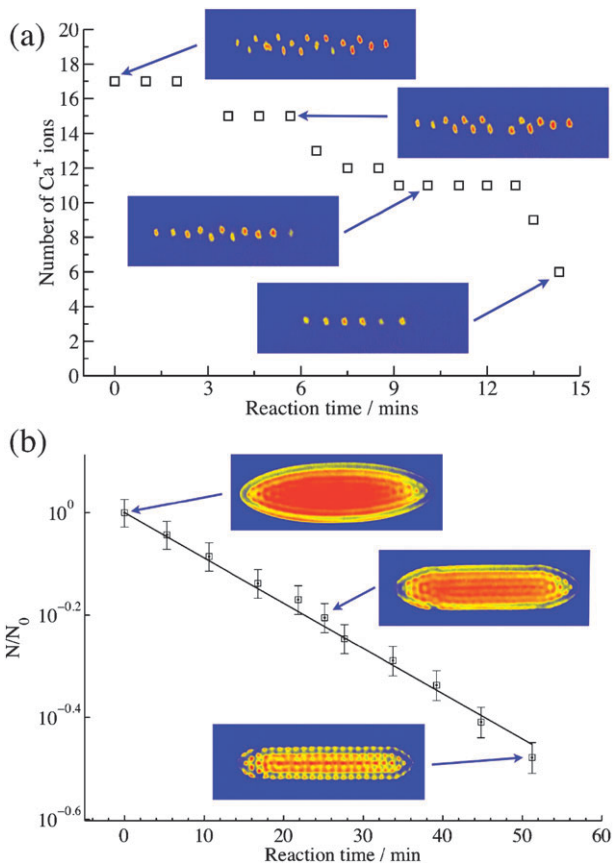

Fig. 6 Cold chemical reactions between laser-cooled Ca^+ ions and velocity-selected CH_3F molecules. (a) Small Coulomb crystals: the progress of reaction can be followed with single-particle sensitivity by monitoring the removal of single Ca^+ ions from the crystal. (b) Large Coulomb crystals: semi-logarithmic plot of the experimentally determined ratio of unreacted Ca^+ ions N/N_0 *vs.* reaction time (squares). The solid line represents a fit of the experimental data to a pseudo-first order rate law, see text for details.

kinetic-energy distribution) down to $\langle E_{kin}\rangle/k_B \approx 1$ K can be produced.[45,70] The experimental velocity distribution is measurable by pulsing the voltage applied to the quadrupole guide and observing the time of flight distribution at a quadrupole mass spectrometer detector. The velocity-selected molecular beam is directed towards the centre of the ion trap allowing cold ion-molecule reactive collisions with the laser-cooled ions to occur. The flux of cold neutrals at the position of the trap centre (approximately 30 mm downstream from the exit of the guide) is of order 10^6–10^7 molecules s^{-1} depending on the quadrupole-guide voltage.

The extremely high sensitivity that can be achieved with this method is demonstrated in Fig. 6(a). In this experiment a small Coulomb crystal of 17 Ca^+ ions was exposed to a flow of velocity-selected fluoromethane (CH_3F) molecules for about 15 minutes at a quadrupole guide voltage of $V_{QUAD} = 5.0$ kV. The Ca^+ ions react with CH_3F according to ref. 73

$$Ca^+ + CH_3F \rightarrow CaF^+ + CH_3. \quad (13)$$

The extent of reaction can be traced from the disappearance of Ca^+ ions from the fluorescence images taken as a function of the reaction time. It can be seen from Fig. 6(a) that in small Coulomb crystals the chemical reaction can be followed at the single-particle level and that the decrease of the number of ions as a function of the reaction time is completely stochastic.

The depth of the ion trap (>1.2 eV under our experimental conditions) ensures the product CaF^+ ions remain confined and are sympathetically cooled by the remaining laser-cooled Ca^+ ions. This can be seen in Fig. 4, which shows the resonant excitation of a Coulomb crystal of 14 ions before and after the reaction. Whereas the mass scan of the initially pure crystal (image shown in (a), spectrum in (c)) shows only one resonance corresponding to Ca^+, the crystal after reaction ((b) and (d)) shows an additional feature at lower excitation frequencies which is attributed to the presence of sympathetically cooled CaF^+ product ions.

For larger crystals, comprising hundreds of ions, the rate of the decrease of the number of Ca^+ ions $N(t)$ over the course of the reaction becomes statistical and follows a pseudo-first-order rate law

$$N(t) = N_0 \exp\{-N_{CH_3F} k_{bi} t\}, \quad (14)$$

where N_0 is the initial number of Ca^+ ions, N_{CH_3F} stands for the number density of fluoromethane molecules at the position of the Coulomb crystal and k_{bi} is the bimolecular reaction-rate constant. This form of rate law applies because the flux of cold neutrals is constant over the duration of the experiment. Fig. 6(b) shows a semi-logarithmic plot of the ratio of unreacted Ca^+ ions N/N_0 in a large Coulomb crystal *vs.* reaction time. The solid line represents a fit of the experimental data (squares) to eqn (14). The quadrupole-guide voltage used in this particular experiment was $V_{QUAD} = 3.0$ kV. The images of the ions taken over the course of the reaction show the characteristic flattening of the Ca^+ core which is indicative of the formation of a bi-component Coulomb crystal with the heavier CaF^+ ions aggregating on the edges. The Coulomb crystals shown in Fig. 6(b) prove to be too large to determine the number of ions by a simple counting procedure. Instead, the ion numbers have been derived from the apparent volume of the crystals (*i.e.*, the volume occupied by the fluorescing Ca^+ ions) and assuming a constant ion density (see Fröhlich *et al.*[74]).

At a quadrupole guide voltage $V_{QUAD} = 3.0$ kV the second-order rate constant was found to be $k_{bi} = 1.3(6) \times 10^{-9}$ cm^3 s^{-1}. This result can be contrasted with the room-temperature value of $k_{bi}(T = 298\ K) = 4.2(4) \times 10^{-10}$ cm^3 s^{-1} and the Langevin rate constant for this reaction $k_{Langevin} = 9.4 \times 10^{-10}$ cm^3 s^{-1}. Although the low-temperature value for the rate constant is in accordance with the Langevin rate within the experimental uncertainty, the room-temperature value is significantly lower as has already been observed in previous studies. A possible reason for this unusually low rate constant is the existence of a low-lying potential-energy barrier along the reaction coordinate which acts as a bottleneck for the reactive flux from the reactants to the products as discussed by Harvey *et al.*[73]

The mean kinetic energy of the velocity-selected molecules can be tuned by adjusting the high voltages applied to the quadrupole guide enabling the determination of rate constants as a function of the collision energy of the reaction partners.[45] Adapting the size and shape of the Coulomb crystal offers yet another possibility to tune the collision energy by varying the kinetic-energy distributions of the ions.[52] Hence, our new method allows the study of ion-molecule reactions over a wide temperature range, down to ≈1 K. Moreover, the method is not restricted to chemical reactions with laser-cooled ions. Roth *et al.* have recently demonstrated that rate constants for reactions with non-fluorescing sympathetically cooled ions can be determined based on an analysis of the reaction-time dependent fluorescence images of multi-component Coulomb crystals using MD simulations.[75]

Although the new approach presented here is in many ways complementary to established methods in the field of low-temperature chemistry in which cold samples are produced in continuous supersonic beams (the CRESU (Cinétique de Réaction en Ecoulement Super-Sonique Uniforme) method, typically down to around 15 K),[76,77] in pulsed molecular beams[78] (≈1 K) or in buffer-gas cooled ion traps[23] (≳10 K), it has considerable scope for further improvements. For instance by replacing the velocity selector with a Stark decelerator as a source for cold neutral molecules (see, *e.g.*, ref. 79 and references therein) one can expect to reach even lower collision energies corresponding to temperatures of tens of mK. In combination with methods to produce state-selected cold molecular ions (see section 4), a fully state-selected ion molecule-collision experiment could be realised which would enable the determination of state- and temperature-dependent reaction-rate constants from room temperature down to the cold regime. At present, experiments along these lines are being developed in our laboratory.

3.3 High-resolution spectroscopy and frequency metrology

Over the past decades laser-cooled atomic ions have been extensively used in ultrahigh-resolution spectroscopic experiments as candidates for new frequency standards and to test fundamental physical concepts such as the time variation of natural constants, see, *e.g.*, ref. 10, 11, 80, 81 and references cited

therein. Indeed, cold trapped ions represent almost ideal systems for frequency-metrology applications: their tight spatial confinement allows spectroscopic experiments on single particles to be performed; their low temperatures lead to a very small Doppler broadening of the spectral lines; and their long storage times enable long-term measurements on the same particle (up to years[11]). Whereas most experiments have thus far been performed on atomic ions, the recent development of sympathetic cooling methods provides the opportunity to perform ultrahigh-resolution spectroscopic studies on cold molecular ions. Such experiments would allow one to address scientific problems such as a possible time variation of the electron-to-proton mass ratio m_e/m_p[82] and the measurement of the energy difference between the two enantiomeric forms of a molecule induced by the parity-violating weak interaction.[83] Apart from applications in frequency metrology, cold samples also represent attractive systems for conventional high-resolution ion spectroscopy because of the markedly reduced Doppler line broadening at very low temperatures. Such studies are of interest in the context of the general theory of the intramolecular dynamics of cations,[84–86] in astrophysics to identify cationic species in space,[25,87] and in biochemistry to elucidate the structure of biologically relevant positively charged biomolecules.[24]

A proof-of-principle experiment was recently performed by Schiller and co-workers, who studied the near-infrared spectrum of cold HD^+ ions sympathetically cooled into a Coulomb crystal, achieving MHz resolution and a frequency accuracy on the ppb level.[88,89] The HD^+ ions were produced by electron-impact ionization and sympathetically cooled by laser-cooled Be^+ ions. The spectra were recorded using a resonance-enhanced multiphoton-dissociation (REMPD) scheme whereby the HD^+ ions were photodissociated using 266 nm cw ultraviolet radiation following the excitation of a rovibrational transition $(v'' = 0, N'') \rightarrow (v' = 4, N')$ at a wavelength near 1.4 μm. v'', N'' and v', N' stand for the vibration–rotation quantum numbers in the ground and excited vibrational states, respectively. To improve the resolution the spectroscopy laser beam was aligned to be collinear with the trap axis in order to minimize Doppler line broadening induced by the micromotion.

The rate of photodissociation of HD^+ ions under the influence of the spectroscopy and dissociation laser fields was taken as a measure of the absorption cross section at the relevant excitation frequency. The HD^+ loss rate was determined from the decrease of the magnitude of the HD^+ signal in repeated resonant-excitation mass scans of the multi-component crystal taken as a function of the time of exposure to the excitation laser beams. Fig. 7 shows the spectra obtained for the two rovibrational transitions $(v'',J'') \rightarrow (v',J') = (0,2) \rightarrow (4,1)$ and $(0,2) \rightarrow (4,3)$. A spectral resolution of order 40 MHz was achieved which enabled the partial resolution of the hyperfine structure of HD^+. The resolution was limited by residual Doppler broadening, which was attributed to the small coupling of the micromotion to the axial motion of the ions.[88] The absolute frequency of the transitions was determined by locking the 1.4 μm diode laser to a GPS-referenced hydrogen maser using a femtosecond frequency comb. In this way the line centres could be determined with an absolute accuracy of 450 kHz or a relative accuracy of 2.3 ppb.[89]

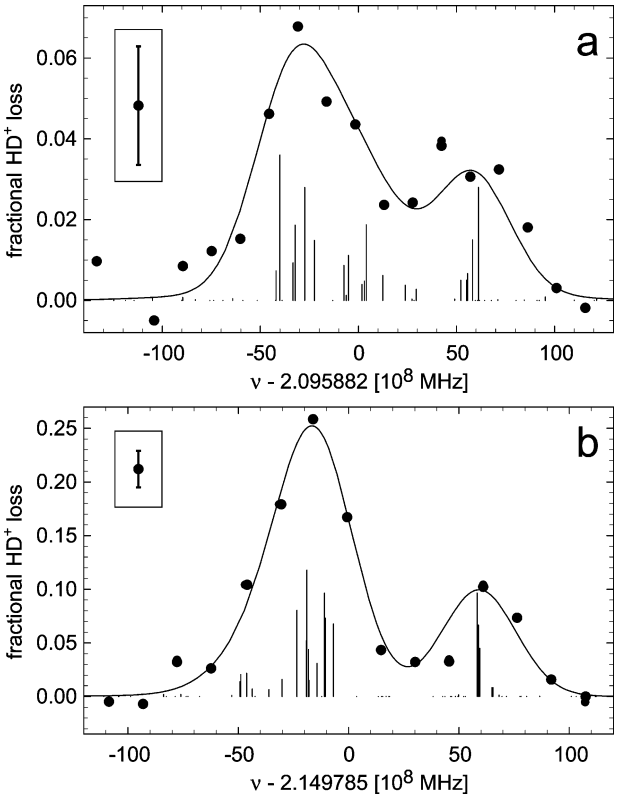

Fig. 7 Resonance-enhanced multiphoton dissociation (REMPD) spectra of HD^+ ions sympathetically cooled into a multi-component Coulomb crystal. The spectra show partially resolved hyperfine structure in the (a) $(v'',J'') \rightarrow (v',J') = (0,2) \rightarrow (4,1)$ and (b) $(0,2) \rightarrow (4,3)$ rovibrational transitions at a resolution of $\approx$40 MHz. The spectra were obtained by measuring the rate of photodissociation of HD^+ ions as a function of the excitation-laser wavelength. Reproduced from Roth *et al.*[88] Copyright 2006 by the American Physical Society.

These studies impressively demonstrate the potential of cold molecular ions for applications in high-resolution spectroscopy. REMPD spectroscopy is a generally applicable technique for ions which exhibit suitable resonantly-enhanced photodissociation pathways, paving the way to study the structure and dynamics of a wide range of molecular cations with unprecedented resolution and sensitivity. The resolution can in principle be further improved by reducing or eliminating first-order Doppler shifts by, *e.g.*, Doppler-free spectroscopy.[90]

4. Outlook

The past years have seen impressive advances in the generation of molecular ions at very low temperatures: the first applications in mass spectrometry, chemistry and spectroscopy demonstrate their considerable scientific potential. However, the field is only in its infancy and the methods developed thus far can be extended in several possible directions to open up the world of cold molecular ions to an even wider range of fascinating applications.

The generation of molecular ions in the motional ground state of the ion trap would enable reactive scattering experiments at even lower temperatures (down to μK) and pave the way to the implementation of ion-trap quantum-logic

protocols using molecular species. Ground-state cooling has already been demonstrated in systems consisting of one laser-cooled and one sympathetically cooled atomic ion.[42,91] The generalisation of these experiments to molecular ions remains to be addressed in the future.

Another important milestone is the production of translationally-cold molecular ions in a well-defined rovibronic quantum state. Indeed, internal-state preparation is desirable, if not essential, for a range of applications such as state-selected low-temperature reactive-collision studies,[45] quantum logic[92] and frequency metrology.[82] Current proposals to address this problem include the optical pumping of the population into one or only a few internal states,[93,94] probabilistic state preparation,[95] and optical coupling of the internal degrees of freedom with the motional degrees of freedom of the ions[96] in a translationally-cold but internally thermalized sample of molecular ions. Another possible strategy aims at producing the molecular ions in a well-defined rovibronic state, *e.g.*, by state-selective photoionization, and preserving this state in the course of sympathetic cooling and for the duration of further experiments.[45] Resonance-enhanced multiphoton-ionization (REMPI) techniques generally show a high degree of selectivity in the final ion states produced, and pulsed field ionization techniques can be even more selective.[97,98]

Finally, for frequency-metrology experiments it is desirable to use a non-destructive detection technique to be able to perform repeated spectroscopic measurements on a single molecular ion over extended periods of time. For sympathetically cooled ions, such a scheme has recently been demonstrated by Schmidt *et al*. in a system consisting of a single Al^+ ion sympathetically cooled by a laser-cooled Be^+ ion using techniques originally developed in the context of ion-trap quantum-information processing.[99] An application of this method to the spectroscopy of sympathetically cooled molecular ions is likely to prove highly challenging because it requires both ground-state cooling of the sympathetically cooled species and its (repeated) preparation in a specific internal quantum state.[82,92]

Although the scope of this outlook is limited to only a few of the possible future developments in the field, it highlights the variety of prospective applications of cold molecular ions in both chemistry and physics.

References

1 C. J. Pethick and H. Smith, *Bose–Einstein Condensation in Dilute Gases*, Cambridge University Press, 2001.
2 R. Combescot, *J. Low Temp. Phys.*, 2006, **145**, 267.
3 *Interactions in Ultracold Gases: From Atoms to Molecules*, ed. M. Weidemüller and C. Zimmermann, Wiley-VCH, Weinheim, 2003.
4 P. F. Weck and N. Balakrishnan, *Int. Rev. Phys. Chem.*, 2006, **25**, 283.
5 J. M. Hutson and P. Soldán, *Int. Rev. Phys. Chem.*, 2006, **25**, 283.
6 J. I. Cirac and P. Zoller, *Phys. Rev. Lett.*, 1995, **74**, 4091.
7 D. DeMille, *Phys. Rev. Lett.*, 2002, **88**, 067901.
8 P. Rabl, D. DeMille, J. M. Doyle, M. D. Lukin, R. J. Schoelkopf and P. Zoller, *Phys. Rev. Lett.*, 2006, **97**, 033003.
9 J. Ye, H. J. Kimble and H. Katori, *Science*, 2008, **320**, 1734.
10 T. Rosenband, D. B. Hume, P. O. Schmidt, C. W. Chou, A. Brusch, L. Lorini, W. H. Oskay, R. E. Drullinger, T. M. Fortier, J. E. Stalnaker, S. A. Diddams, W. C. Swann, N. R. Newbury, W. M. Itano, D. J. Wineland and J. C. Bergquist, *Science*, 2008, **319**, 1808.
11 S. Bize, S. A. Diddams, U. Tanaka, C. E. Tanner, W. H. Oskay, R. E. Drullinger, T. E. Parker, T. P. Heavner, S. R. Jefferts, L. Hollberg, W. M. Itano and J. C. Bergquist, *Phys. Rev. Lett.*, 2003, **90**, 150802.
12 J. Ye, S. Blatt, M. M. Boyd, S. M. Foreman, E. R. Hudson, T. Ido, B. Lev, A. D. Ludlow, B. C. Sawyer, B. Stuhl and T. Zelevinsky, in *AIP Conference Proceedings*, ed. C. Roos, H. Häffner and R. Blatt, American Institute of Physics, 2006, vol. CP869, p. 80.
13 B. E. Sauer, H. T. Ashworth, J. J. Hudson, M. R. Tarbutt and E. A. Hinds, in *AIP Conference Proceedings*, ed. C. Roos, H. Häffner and R. Blatt, American Institute of Physics, 2006, vol. CP869, p. 44.
14 M. Drewsen, I. Jensen, J. Lindballe, N. Nissen, R. Martinussen, A. Mortensen, P. Staanum and D. Voigt, *Int. J. Mass Spectrom.*, 2003, **229**, 83.
15 E. Wigner, *Phys. Rev. A*, 1934, **46**, 1002.
16 S. Ichimaru, *Rev. Mod. Phys.*, 1982, **54**, 1017.
17 D. H. E. Dubin and T. M. O'Neill, *Rev. Mod. Phys.*, 1999, **71**, 87.
18 E. L. Pollock and J. P. Hansen, *Phys. Rev. A*, 1973, **8**, 3110.
19 R. W. Hasse and J. P. Schiffer, *Ann. Phys.*, 1990, **203**, 419.
20 F. Diedrich, E. Peik, J. M. Chen, W. Quint and H. Walther, *Phys. Rev. Lett.*, 1987, **59**, 2931.
21 D. J. Wineland, J. C. Bergquist, W. M. Itano, J. J. Bollinger and C. H. Manney, *Phys. Rev. Lett.*, 1987, **59**, 2935.
22 H. J. Metcalf and P. van der Straten, *Laser Cooling and Trapping*, Springer, New York, 1999.
23 D. Gerlich, *Phys. Scr.*, 1995, **T59**, 256.
24 O. V. Boyarkin, S. R. Mercier, A. Kamariotis and T. R. Rizzo, *J. Am. Chem. Soc.*, 2006, **128**, 2816.
25 A. Dhzonson and J. P. Maier, *Int. J. Mass Spectrom.*, 2006, **255–256**, 139.
26 A. Steane, *J. Phys. B: At. Mol. Opt. Phys.*, 1997, **64**, 623.
27 F. Schmidt-Kaler, H. Häffner, S. Gulde, M. Riebe, G. P. T. Lancaster, T. Deuschle, C. Becher, W. Hänsel, J. Eschner, C. F. Roos and R. Blatt, *Appl. Phys. B*, 2003, **77**, 789.
28 R. Blatt and D. Wineland, *Nature*, 2008, **453**, 1008.
29 T. Baba and I. Waki, *Jpn. J. Appl. Phys.*, 1996, **35**, L1134.
30 K. Molhave and M. Drewsen, *Phys. Rev. A*, 2000, **62**, 011401.
31 J. D. Prestage, G. J. Dick and L. Maleki, *J. Appl. Phys.*, 1989, **66**, 1013.
32 D. J. Berkeland, J. D. Miller, J. C. Bergquist, W. M. Itano and D. J. Wineland, *J. Appl. Phys.*, 1998, **83**, 5025.
33 M. Drewsen and A. Brøner, *Phys. Rev. A*, 2000, **62**, 045401.
34 W. M. Itano, J. J. Bollinger, J. N. Tan, B. Jelenković, X.-P. Huang and D. J. Wineland, *Science*, 1998, **279**, 686.
35 K. Koo, J. Sudbery, D. M. Segal and R. C. Thompson, *Phys. Rev. A*, 2004, **69**, 043402.
36 K. Okada, K. Yasuda, T. Takayanagi, M. Wada, H. A. Schuessler and S. Ohtani, *Phys. Rev. A*, 2007, **75**, 033409.
37 D. Stick, W. K. Hensinger, S. Olmschenk, M. J. Madsen, K. Schwab and C. Monroe, *Nat. Phys.*, 2006, **2**, 36.
38 R. E. March and J. F. Todd, *Quadrupole Ion Trap Mass Spectrometry*, John Wiley & Sons, 2nd edn, 2005.
39 P. K. Ghosh, *Ion Traps*, Clarendon Press, 1995.
40 D. Gerlich, *Adv. Chem. Phys.*, 1992, **82**, 1.
41 H. G. Dehmelt, *Adv. At. Mol. Phys.*, 1967, **3**, 53.
42 M. D. Barrett, B. Demarco, T. Schaetz, V. Meyer, D. Leibfried, J. Britton, J. Chiaverini, W. M. Itano, B. Jelenković, J. D. Jost, C. Langer, T. Rosenband and D. J. Wineland, *Phys. Rev. A*, 2003, **68**, 042302.
43 B. Roth, P. Blythe, H. Daerr, L. Patacchini and S. Schiller, *J. Phys. B: At. Mol. Opt. Phys.*, 2006, **39**, S1241.
44 P. Bowe, L. Hornekaer, C. Brodersen, M. Drewsen, J. S. Hangst and J. P. Schiffer, *Phys. Rev. Lett.*, 1999, **82**, 2071.
45 S. Willitsch, M. Bell, A. Gingell, S. R. Procter and T. P. Softley, *Phys. Rev. Lett.*, 2008, **100**, 043203.
46 B. Roth, A. Ostendorf, H. Wenz and S. Schiller, *J. Phys. B: At. Mol. Opt. Phys.*, 2005, **38**, 3673.
47 D. Leibfried, R. Blatt, C. Monroe and D. Wineland, *Rev. Mod. Phys.*, 2003, **75**, 281.
48 A. Mortensen, E. Nielsen, T. Matthey and M. Drewsen, *Phys. Rev. Lett.*, 2006, **96**, 103001.

49 J. P. Schiffer, M. Drewsen, J. S. Hangst and L. Hornekaer, *Proc. Natl. Acad. Sci. U. S. A.*, 2001, **97**, 10697.
50 J. P. Schiffer, *J. Phys. B: At. Mol. Opt. Phys.*, 2003, **36**, 511.
51 C. B. Zhang, D. Offenberg, B. Roth, M. A. Wilson and S. Schiller, *Phys. Rev. A*, 2007, **76**, 012719.
52 M. Bell, A. Gingell, J. Oldham, T. P. Softley and S. Willitsch, in preparation.
53 M. A. van Eijkelenborg, M. E. M. Storkey, D. M. Segal and R. C. Thompson, *Phys. Rev. A*, 1999, **60**, 3903.
54 A. Ostendorf, C. B. Zhang, M. A. Wilson, D. Offenberg, B. Roth and S. Schiller, *Phys. Rev. Lett.*, 2006, **97**, 243005.
55 L. Hornekær, N. Kjærgaard, A. M. Thommesen and M. Drewsen, *Phys. Rev. Lett.*, 2001, **86**, 1994.
56 T. Baba and I. Waki, *J. Chem. Phys.*, 2002, **116**, 1858.
57 T. Baba and I. Waki, *J. Appl. Phys.*, 2002, **92**, 4109.
58 T. Baba and I. Waki, *Appl. Phys. B*, 2002, **74**, 375.
59 T. Matthey, J. P. Hansen and M. Drewsen, *Phys. Rev. Lett.*, 2003, **91**, 165001.
60 A. Bertelsen, S. Jorgensen and M. Drewsen, *J. Phys. B: At. Mol. Opt. Phys.*, 2006, **39**, L83.
61 J. C. J. Koelemeij, B. Roth and S. Schiller, *Phys. Rev. A*, 2007, **76**, 023413.
62 B. Roth, P. Blythe and S. Schiller, *Phys. Rev. A*, 2007, **75**, 023402.
63 M. Drewsen, A. Mortensen, R. Martinussen, P. Staanum and J. L. Sorensen, *Phys. Rev. Lett.*, 2004, **93**, 243201.
64 M. Redshaw, J. McDaniel and E. G. Myers, *Phys. Rev. Lett.*, 2008, **100**, 093002.
65 K. Højbjerre, D. Offenberg, C. Z. Bisgaard, H. Stapelfeldt, P. F. Staanum, A. Mortensen and M. Drewsen, *Phys. Rev. A*, 2008, **77**, 030702.
66 P. F. Staanum, K. Højbjerre, R. Wester and M. Drewsen, *Phys. Rev. Lett.*, 2008, **100**, 243003.
67 E. I. Dashevskaya, A. I. Maergoiz, J. Troe, I. Litvin and E. E. Nikitin, *J. Chem. Phys.*, 2003, **118**, 7313.
68 J. M. Hutson and P. Soldán, *Int. Rev. Phys. Chem.*, 2006, **25**, 497.
69 R. V. Krems, *Phys. Chem. Chem. Phys.*, 2008, **10**, 4079.
70 S. A. Rangwala, T. Junglen, T. Rieger, P. W. H. Pinkse and G. Rempe, *Phys. Rev. A*, 2003, **67**, 043406.
71 T. Rieger, T. Junglen, S. A. Rangwala, G. Rempe, P. W. H. Pinkse and J. Bulthuis, *Phys. Rev. A*, 2006, **73**, 061402.
72 M. Motsch, M. Schenk, L. D. van Buuren, M. Zeppenfeld, P. W. H. Pinkse and G. Rempe, *Phys. Rev. A*, 2007, **76**, 061402.
73 J. N. Harvey, D. Schröder, W. Koch, D. Danovich, S. Shaik and H. Schwarz, *Chem. Phys. Lett.*, 1997, **273**, 164.
74 U. Fröhlich, B. Roth and S. Schiller, *Phys. Plasmas*, 2005, **12**, 073506.
75 B. Roth, P. Blythe, H. Wenz, H. Daerr and S. Schiller, *Phys. Rev. A*, 2006, **73**, 042712.
76 B. R. Rowe, A. Canosa and V. Le Page, *Int. J. Mass Spectrom. Ion Processes*, 1995, **149/150**, 573.
77 I. W. M. Smith, *Angew. Chem., Int. Ed.*, 2006, **45**, 2842.
78 M. A. Smith, *Int. Rev. Phys. Chem.*, 1998, **17**, 35.
79 H. L. Bethlem and G. Meijer, *Int. Rev. Phys. Chem.*, 2003, **22**, 73.
80 J.-P. Uzan, *Rev. Mod. Phys.*, 2003, **75**, 403.
81 L. Hollberg, C. W. Oates, G. Wilpers, C. W. Hoyt, Z. W. Barber, S. A. Diddams, W. H. Oskay and J. C. Bergquist, *J. Phys. B: At. Mol. Opt. Phys.*, 2005, **38**, S469.
82 S. Schiller and V. Korobov, *Phys. Rev. A*, 2005, **71**, 032505.
83 M. Quack, J. Stohner and M. Willeke, *Annu. Rev. Phys. Chem.*, 2008, **59**, 741.
84 S. Willitsch, U. Hollenstein and F. Merkt, *J. Chem. Phys.*, 2004, **120**, 1761.
85 S. Willitsch, F. Innocenti, J. M. Dyke and F. Merkt, *J. Chem. Phys.*, 2005, **122**, 024311.
86 S. Willitsch, Ch. Jungen and F. Merkt, *J. Chem. Phys.*, 2006, **124**, 204312.
87 E. Herbst, *Chem. Soc. Rev.*, 2001, **30**, 168.
88 B. Roth, J. C. J. Koelemeij, H. Daerr and S. Schiller, *Phys. Rev. A*, 2006, **74**, 040501.
89 J. C. J. Koelemeij, B. Roth, A. Wicht, I. Ernsting and S. Schiller, *Phys. Rev. Lett.*, 2007, **98**, 173002.
90 W. Demtröder, *Laser Spectroscopy*, Springer, Berlin, 3rd edn, 2003.
91 H. Rohde, S. T. Gulde, C. F. Roos, P. A. Barton, D. Leibfried, J. Eschner, F. Schmidt-Kaler and R. Blatt, *J. Opt. B*, 2001, **3**, S34.
92 P. O. Schmidt, T. Rosenband, J. C. J. Koelemeij, D. B. Hume, W. M. Itano, J. C. Bergquist and D. J. Wineland, in *AIP Conference Proceedings*, ed. M. Drewsen, U. Uggerhoj and H. Knudsen, American Institute of Physics, 2006, vol. CP862, p. 305.
93 I. S. Vogelius, L. B. Madsen and M. Drewsen, *Phys. Rev. Lett.*, 2002, **89**, 173003.
94 I. S. Vogelius, L. B. Madsen and M. Drewsen, *J. Phys. B: At. Mol. Opt. Phys.*, 2004, **37**, 4571.
95 I. S. Vogelius, L. B. Madsen and M. Drewsen, *J. Phys. B: At. Mol. Opt. Phys.*, 2006, **39**, S1259.
96 I. S. Vogelius, L. B. Madsen and M. Drewsen, *J. Phys. B: At. Mol. Opt. Phys.*, 2006, **39**, S1267.
97 S. Willitsch and F. Merkt, *Int. J. Mass Spectrom.*, 2005, **245**, 14.
98 H. Dickinson, D. Rolland and T. P. Softley, *Philos. Trans. R. Soc. London, Ser. A*, 1997, **355**, 1585.
99 P. O. Schmidt, T. Rosenbrand, C. Langer, W. M. Itano, J. C. Bergquist and D. J. Wineland, *Science*, 2005, **309**, 749.

